Journal of Pathology
J Pathol 2025
Published online 3 October 2025 in Wiley Online Library
(wileyonlinelibrary.com) DOI: 10.1002/path.6468

ORIGINAL ARTICLE

Androgen receptor–mediated regulation of BRCA1 modulates the antioxidant defense in prostate cancer

Saiganesh Sriraman[1†], Verneri Virtanen[1†], Antti Kukkula[1], Mervi Toriseva[1], Anni Lumiainen[1], Gun West[1,2], Matti Poutanen[3,4], Pekka Taimen[1,2,5] and Maria Sundvall[1,6*]

[1] *Cancer Research Unit, Institute of Biomedicine, and FICAN West Cancer Center Laboratory, University of Turku and Turku University Hospital, Turku, Finland*
[2] *InFLAMES Research Flagship Center, University of Turku and Åbo Akademi University, Turku, Finland*
[3] *Research Centre for Integrative Physiology and Pharmacology, Institute of Biomedicine, and FICAN West Cancer Center, University of Turku, Turku, Finland*
[4] *Institute of Medicine, Sahlgrenska Academy at University of Gothenburg, Gothenburg, Sweden*
[5] *Department of Pathology, Tyks Laboratories, Turku University Hospital, Turku, Finland*
[6] *Department of Oncology, Turku University Hospital, Turku, Finland*

**Correspondence to: M Sundvall, Cancer Research Unit, Institute of Biomedicine, FICAN West Cancer Center Laboratory, University of Turku and Turku University Hospital, Kiinamyllynkatu 10, 20520, Turku, Finland. E-mail: mahesu@utu.fi*

[†]These authors contributed equally to this work.

Abstract

Lethal prostate cancer (PCa) is a genetically heterogeneous disease characterized by evolving androgen receptor (AR) signaling, eventually culminating in castration resistance. The tumor suppressor gene *BRCA1* has multiple functions that include secondary processes cooperating with its main function as a caretaker of genomic integrity. *BRCA1* is often mutated in breast and ovarian cancer, but *BRCA1* mutations are also associated with PCa, although they are less frequently observed. Most PCa patients do not, however, carry *BRCA1* mutations, and interestingly, it has been shown that *BRCA1* expression is enriched in castration-resistant PCa. In this study we elucidated the prostate tissue-specific role of the BRCA1 protein. Although the regulation of DNA damage response genes has been studied in PCa, comprehensive analyses of *BRCA1* regulation in the context of androgen signaling are lacking. Our results indicate that *BRCA1* is dynamically regulated by AR signaling and that activation of AR via its natural ligand, dihydrotestosterone, represses BRCA1 expression. Our analyses both *in vitro* and of patient samples and mouse xenografts showed that BRCA1 expression was induced and sustained after androgen deprivation. Moreover, we observed that oxidative stress–related pathways were regulated by BRCA1 in PCa cells and that androgen deprivation therapy–induced activation of BRCA1 supported the function of NRF2, the master regulator of antioxidant defense, and a known interactor of BRCA1. Impaired NRF2 activity, in the absence of BRCA1, decreased growth in a 3D environment. Our findings shed light on the functional role of BRCA1 protein in PCa and suggest that *BRCA1* is regulated by the evolving AR signaling state during PCa progression. Thus, AR-mediated suppression of *BRCA1* accumulates oncogenic alterations in the early phases of PCa tumor progression and safeguards from excessive reactive oxygen species (ROS) when upregulated during androgen deprivation therapy.

Keywords: castration-resistant prostate cancer; androgen deprivation therapy; androgen receptor; BRCA1; DNA damage; oxidative stress; NRF2

Received 13 March 2025; Revised 14 June 2025; Accepted 7 August 2025

No conflicts of interest were declared.

Introduction

BRCA1 is a tumor suppressor that supports genomic integrity via its central role in DNA damage response (DDR), where it is specifically involved in the repair of double-strand DNA breaks by homologous recombination (HR) [1]. Therefore, when BRCA1 function is lost, somatic oncogenic alterations are more likely to become incorporated in the DNA, consequently inducing carcinogenesis or cancer progression [1]. In addition, BRCA1 functions as a transcriptional factor and part of a ubiquitin ligase complex and has pleiotropic roles in cells pertaining to the cell cycle, centrosome function, and the immune system [1,2]. In keeping with the connection to various essential functions, as well as the role in maintaining genomic integrity, *BRCA1* knockout is

embryonically lethal, *BRCA1* germline mutations are heterozygous, and *BRCA1* somatic mutations require the presence of an accompanying mutation such as p53 [1,2]. BRCA1 also prevents the degradation of the master regulator for antioxidant response, nuclear factor erythroid 2-related factor 2 (NRF2) [3–5]. This secondary effect cooperates with the tumor suppressor gene function by protecting cells against reactive oxygen species (ROS), thereby supporting genomic integrity [5].

DDR genes are frequently mutated in prostate cancer (PCa), with alterations observed in up to 20–30% of castration-resistant PCa (CRPC) cases [6–8]. Most mutations target *BRCA2* and *BRCA1* mutations and are only found in 1%–2% of patients [6,7,9–11]. Previous preclinical studies have demonstrated an interplay between androgen receptor (AR) signaling and DDR in PCa [12–16]. However, the results are contradictory, and the interpretation of these findings remains complex. For instance, while influential work in the field has suggested that AR activation promotes DDR, data from major PCa patient datasets appear to paradoxically indicate that *BRCA1* expression is enriched in CRPC [13,17,18]. Adding to this complexity, the antiandrogen enzalutamide decreases BRCA1 expression in preclinical models [13]. Importantly, the regulation of BRCA1 protein by AR by its natural ligands or by androgen deprivation (AD) has not been reported. Most studies have instead relied on a limited number of synthetic androgens, AR inhibitors, or small RNAs instead of systematic physiological approaches, or they have reported effects on DDR genes but excluded *BRCA1* [12–16].

Here, we characterized the regulation of BRCA1 by AR signaling using a panel of cell lines, patient samples, and a mouse xenograft model of AD therapy (ADT) and studied the implications of this regulation by exploring the tissue-specific role of BRCA1 protein in PCa. We discovered that AR activation is a repressor of *BRCA1* transcription, and conversely, BRCA1 expression is sustained in response to AD. Furthermore, we showed that PCa hijacks a BRCA1-NRF2 regulatory axis to implement an antioxidant response against ROS generated by AD, enabling PCa progression.

Materials and methods

Ethics approval

The use of patient tissue material was approved by the Ethics Committee of the Hospital District of Helsinki and Uusimaa (84/13/03/00/2014; §3 30.01.2015), the Hospital District of Southwest Finland (number T206/2014), and the National Supervisory Authority for Welfare and Health (VALVIRA, 8008/06.01.03/2014).

Cell culture and treatments

PC-3, VCaP, LNCaP, and 22Rv1 cells (ATCC, Manassas, VA, USA) were cultured in the presence of 1% penicillin–streptomycin solution (Sigma-Aldrich, St. Louis, MO, USA), except during the experiments, routinely tested to be mycoplasma-free and checked for authenticity, as previously described [19].

AD was performed using phenol-red free media containing 5% charcoal-stripped FBS (Gibco, Waltham, MA, USA; AD media [ADM]). Normal culture conditions were used as controls for deprivation experiments and are referred to as control media (CM). Dihydrotestosterone (DHT; Sigma-Aldrich) and R1881 (Sigma-Aldrich) were used to stimulate AR after incubation in ADM for 48 h by incubating for 24 h prior to lysis unless specified otherwise. Cell proliferation (confluence) in a 2D culture was monitored in real time for up to 72 h using IncuCyte S3 (Sartorius, Göttingen, Germany) 24 h after transfection. MTS cell viability assay was done as previously described [19].

RNA interference and transfection

Transfection was performed using *Silencer*® Select siRNA oligonucleotides (Ambion, Austin, TX, USA), which are listed, together with the percentage and type of Dharmafect reagent (Horizon Discovery, Waterbeach, UK), in the supplementary material, Table S1 as previously described [19].

Organotypic 3D growth assays

PC-3 and LNCaP cells were grown in 3D as previously described [19]. The multispheroid average area was measured using 10 wells from each condition using the IncuCyte S3 multispheroid analysis software (Sartorius). Cell recovery solution (Corning® Cell Recovery Solution, Sigma-Aldrich) was added following the manufacturer's protocol to extract the organoids from the basement membrane matrix prior to lysis.

Cell lysis and immunoblotting

Cells were lysed and western blotting was performed as previously described [19]. Equal amounts of 30–100 µg of total protein from the lysate supernatants were analyzed. The antibodies used are listed in the supplementary material, Table S2.

RT-qPCR

The isolated RNA was concentrated, and its purity and concentration were assessed before cDNA synthesis, following the manufacturer's protocol. RT-qPCR was then performed using TaqMan™ Fast Advanced Master Mix (Thermo Fisher Scientific, Waltham, Massachusetts, USA). The TaqMan™ Gene Expression Assay (FAM) probes used in the assay are listed in the supplementary material, Table S3. Additional details are provided in the Supplementary Materials and Methods.

Murine VCaP xenografts of early ADT response

VCaP xenograft sections were generated according to a previously described protocol and permissions [20]. Subcutaneous tumors were grown for 4 weeks, and surgical castration was performed. The mice were

sacrificed either 2 days (Cas 2D) or 5 days (Cas 5D) after castration. The Intact group, serving as the noncastrated control, was sacrificed 5 days after the surgery in the treatment groups. Tumors generated under these conditions were collected and fixed in formalin, followed by sectioning and sample preparation.

Immunohistochemistry (IHC) and digital image analyses

Tissue sections from patient samples in a tissue microarray and from tumor xenografts were deparaffinized with xylene (3 × 7 min) and rehydrated in absolute ethanol (2 × 2 min) and 96% ethanol (2 × 2 min), followed by three washes with distilled water. Antigen retrieval was performed in citrate buffer (pH 6) using a microwave for 7 min at 600 W, 7 min at 450 W, and the sections were left to cool down for 20 min. For pBRCA1 and γH2Ax staining, antigen retrieval was performed using a decloaking chamber (Biocare Medical NxGen, Pacheco, CA, USA) for 20 min. After three washes with distilled water, sections were blocked with 3% hydrogen peroxide for 10 min at room temperature (RT), washed with Tris–HCl buffer, followed by pre-protein blocking in antibody diluent for 10 min at RT, and incubated using antibodies and concentrations specified in the supplementary material, Table S2 for 60 min at RT. After washing with Tris–HCl buffer, the sections were incubated with secondary antibody for 30 min at RT and washed again with Tris–HCl buffer. DAB (Immunologic, WellMed BV, Duiven, the Netherlands) incubation was washed with distilled water after 10 min at RT, and the sections were counterstained with Mayer's hematoxylin (Sigma-Aldrich) for 1 min at RT, followed by washing with distilled water, dehydration twice in 96% ethanol, twice in absolute ethanol, and three times in xylene.

Slides were scanned using a Pannoramic P1000 slide scanner (3DHISTECH, Budapest, Hungary). Xenograft whole-tumor sections were measured for total tumor area in QuPath v0.4.4 (open-source software available from https://qupath.github.io/) using a pixel classifier after refining the area analyzed using manual segmentation. Areas with strong staining were detected using a QuPath pixel classifier. For patient samples, two researchers independently performed manual scoring.

In silico analyses

The effects of R1881 on *BRCA1* and *KLK3* (which encodes prostate-specific antigen [PSA]) mRNA expression in LNCaP cells were analyzed using the GSE50936 dataset [21]. Expression data (log2) were downloaded from the R2: Genomics Analysis and Visualization Platform (http://r2.amc.nl).

Differentially expressed genes were analyzed from the GSE162225 [22] dataset containing RNA-seq data of sh-control and sh-BRCA1 samples of LNCaP cells. Sh1-BRCA1 ($n = 3$) and sh2-BRCA1 (n = 3) samples were pooled and compared to sh-control ($n = 3$) samples, and the data were downloaded from the GEO2R platform at https://www.ncbi.nlm.nih.gov/geo/geo2r/. Volcano plots of differentially expressed genes were generated with VolcaNoseR [23] at https://huygens.science.uva.nl/VolcaNoseR/ using an FDR/adjusted p-value <0.001 (Benjamini–Hochberg) and log2 fold change >1 as the threshold for statistical significance. The lists of the top 500 downregulated genes (supplementary material, Table S4) were compared to the Molecular Signatures Database (MsigDB) (v2024.1) Gene Ontology: Biological Processes (GO:BP), Hallmark and Oncogenic gene set collections at https://www.gsea-msigdb.org/gsea/msigdb to identify significant overlaps with gene sets ($p < 0.05$, FDR < 0.05).

Data of genetic alterations of *BRCA1*, association of expression with clinical features, coexpression analyses of PCa patient and patient-derived organoid datasets, and survival analyses of patients were extracted from cBioPortal at https://www.cbioportal.org/.

Statistical analysis

Statistical analyses were performed using R Studio (open-source software available from https://www.posit.co/) and GraphPad Prism 10.1.2 (GraphPad Software, San Diego, CA, USA). Data extracted from cBioPortal v4.1.9 were generated using the default methods. Spearman's rank correlation coefficient was used to analyze correlations. Two-tailed unpaired Student's t-test or Mann–Whitney U test were used for comparisons between two groups. Analysis of variance (ANOVA) test was used to analyze the differences between the means of more than two groups.

Results

AR activation by DHT and R1881 represses *BRCA1* transcription

In this study we used the PCa cell lines VCaP (*AR*-amplified, *TP53*-mutated, *TMPRSS2-ERG* fusion), LNCaP (*AR*-mutated, *CHEK2*-SNV, *PTEN* loss), 22Rv1 (*AR* splice variant, *BRCA2*-mutated, *ATM*-SNV, *TP53*-mutated, *TMPRSS2–ERG* fusion), and PC-3 (AR-negative, *PTEN* loss) [24]. Thus, three AR-positive cell lines with different AR signaling statuses were used.

To study BRCA1 protein levels in response to AR activation, we first pretreated the highly AR-responsive VCaP cell line with AD mimicking conditions for 96 h. During the last 24, 48, and 72 h of this period, we further stimulated the cells with different DHT concentrations (0.05–10 nM), and all cells were lysed at the 96-h timepoint. DHT treatment increased the levels of AR transcriptional target proteins PSA and FKBP5 at concentrations between 0.5–10 nM (Figure 1A,B). In contrast, BRCA1 protein was downregulated in a dose-dependent manner. As a readout of DNA damage, γH2Ax was downregulated, particularly at later timepoints. Another essential HR protein, Rad51, was also downregulated. These results suggested that unlike the

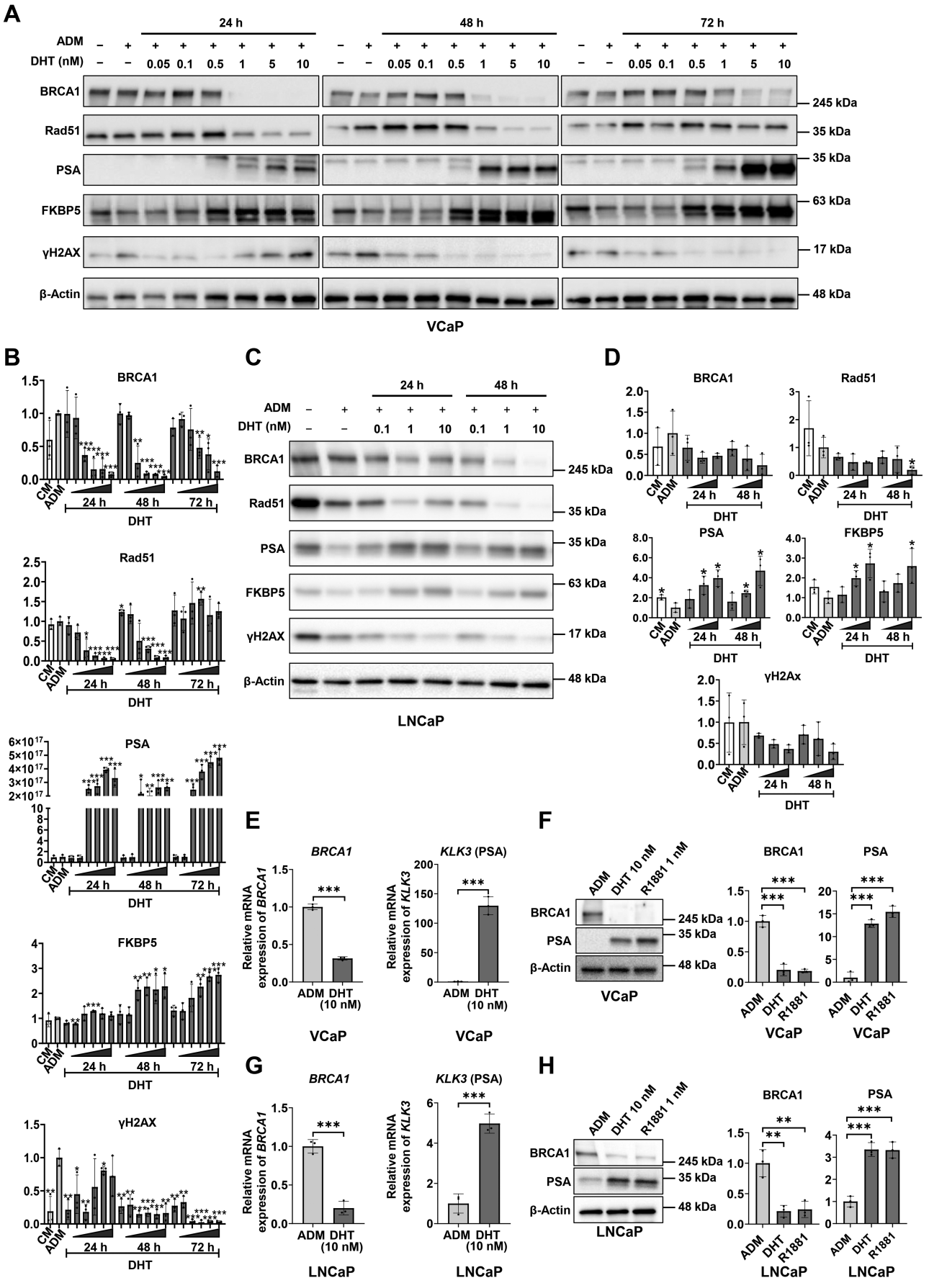

Figure 1 Legend on next page.

protein products of AR target genes KLK3 and FKBP5, BRCA1 and Rad51 expression levels were downregulated in contrast to previous reports of AR activation inducing DDR gene expression.

Stimulation of AR signaling was performed similarly in LNCaP cells (Figure 1C,D). As expected for a cell line with a lower degree of AR amplification, PSA and FKBP5 responses were less extreme, yet highly dose-dependent, while the trends matched the results with VCaP cells for all readouts, and only Rad51 reached significance. These results imply that, unlike known target genes, the HR proteins BRCA1 and Rad51 were not upregulated after stimulating the AR with a natural ligand.

We also examined the correlation between *BRCA1* and AR transcriptional target mRNAs in PCa patient, patient-derived organoid, and patient-derived xenograft datasets [6,9,18,25–27] (supplementary material, Figure S1A,B). The datasets showed a trend of negative correlation, further supporting a possible repressive function of AR activation over *BRCA1*.

Next, we wanted to determine how AR activation mediated BRCA1 downregulation. BRCA1 seemed to be oppositely regulated at similar doses and timepoints as the upregulated AR targets, suggesting that *BRCA1* was regulated by AR activation at the transcriptional level. To test this, we performed RT-qPCR in VCaP cells subjected to 10 nM DHT or vehicle after AD and observed downregulated *BRCA1* mRNA levels in response to AR stimulation (Figure 1E). Synthetic androgen R1881 (1 nM) also downregulated BRCA1 in VCaP cells in a comparable manner to DHT (Figure 1F). Similarly, significant reductions were observed in LNCaP cells (Figure 1G,H). A response in *BRCA1* mRNA to R1881 was also observed by analyzing a published RNA dataset [21] (supplementary material, Figure S1C). This suggested that AR activation repressed *BRCA1* by suppressing its transcription.

AD induces DNA damage and activates BRCA1 in PCa cells

We used media supplemented with a steroid-free serum to deprive AR of its ligand in order to mimic ADT. As expected, VCaP and LNCaP cells showed downregulation of PSA, while 22Rv1, with high AR-V7 expression, retained PSA expression (Figure 2A–D).

We observed upregulation of total BRCA1 in VCaP and LNCaP cells under AD conditions, suggesting that AR-mediated repression of *BRCA1* was abolished upon AD (Figure 2A–C; supplementary material, Figure S2A,B). In contrast, this effect appeared transient in the LNCaP cells, but sustained in VCaP cells. In 22Rv1 cells with no clear PSA response to AD, BRCA1 levels were constant, suggesting that *BRCA1* remained repressed by constitutive AR-V7 activation (Figure 2A,D; supplementary material, Figure S2C). This supported the conclusion that BRCA1 protein levels are linked to AR activity. We observed upregulated γH2Ax and cleaved caspase-3 levels in all cell lines, notably also in the 22Rv1 cell line (Figure 2A–D). We also observed increased levels of phosphorylated BRCA1 (pBRCA1) [28] in all cell lines, indicative of its activation. This suggested that the regulation of BRCA1 activation was separate from the regulation of its expression and might have been induced by AD-related DNA-damaging processes in PCa.

Rad51 was observed to have a trend of downregulation in all cell lines, reaching significance in VCaP and 22Rv1 cells (Figure 2A–D). This suggested that Rad51, unlike BRCA1, did not have a simple inverse correlation with AR activation.

S6 and Akt, as readouts of the PI3K-Akt/mTOR signaling pathway involved in the regulation of cell growth, survival, and protein synthesis, showed an initial surge of phosphorylation in response to AD, but were strongly dephosphorylated at later timepoints in VCaP and 22Rv1 cells (Figure 2A–D; supplementary material, Figure S2A–C). Not surprisingly, this pattern was not present for Akt and barely detectable for phosphorylated S6 (pS6) in LNCaP cells, where constitutive Akt activation due to PTEN loss likely limits further phosphorylation.

Taken together, our results demonstrated that BRCA1 levels were induced in conditions that showed PSA decrease, further supporting the idea that AR activation mediates the repression of BRCA1 levels. Also, γH2Ax, cleaved caspase-3, and pBRCA1 were induced by AD in all cell lines independently of PSA response. This suggested that AR regulates *BRCA1* expression, while BRCA1 phosphorylation appeared to be initiated

Figure 1. BRCA1 and Rad51 expression is repressed by AR activation. (A) Representative western blotting of BRCA1, Rad51, PSA, FKBP5, γH2Ax, and β-actin (loading control) expression in VCaP cells treated with DHT (0.05–10 nM) for 24, 48, and 72 h after preincubation in ADM for 96 h before lysis. Vehicle (methanol) and ADM (96 h) were used as controls. (B) Bar graphs depicting pooled western blotting densitometry results of three independent biological repeats in VCaP cells. Statistical comparisons were performed relative to ADM. (C) Representative western blotting of LNCaP cells treated with DHT (0.1–10 nM) for 24 h, and 48 h after preincubation in ADM for 96 h before lysis with vehicle (methanol) and ADM (96 h) as controls. (D) Bar graphs depicting pooled western blotting densitometry results of three independent biological repeats in LNCaP cells. (E) Bar graphs depicting relative expression of *BRCA1* and *KLK3* (gene encoding PSA) mRNA by RT-qPCR in VCaP cells subjected to ADM for 72 h or DHT (10 nM) for 24 h after 48 h of ADM. (F) Representative western blotting and bar graphs of BRCA1, PSA, and loading control expression in VCaP cells subjected to 72 h of ADM, 24 h of DHT (10 nM), and 24 h R1881 (1 nM) treatments after 48 h of ADM. Vehicle (methanol and/or ethanol) were added to wells not containing DHT and/or R1881, respectively. (G) Bar graphs depicting relative expression of *BRCA1* and *KLK3* mRNA by RT-qPCR in LNCaP cells subjected to ADM for 72 h or DHT (10 nM) for 24 h after 48 h of ADM. (H) Representative western blotting and bar graphs of BRCA1, PSA, and loading control expression in LNCaP cells subjected to 72 h of ADM, 24 h of DHT (10 nM), and 24 h R1881 (1 nM) treatments following 48 h of ADM. Control wells that did not receive DHT or R1881 were treated with the corresponding vehicle (methanol for DHT and ethanol for R1881). The mean and SD from three experiments are represented as bar graphs (*$p < 0.05$, **$p < 0.01$, and ***$p < 0.001$ as determined by Student's *t*-test).

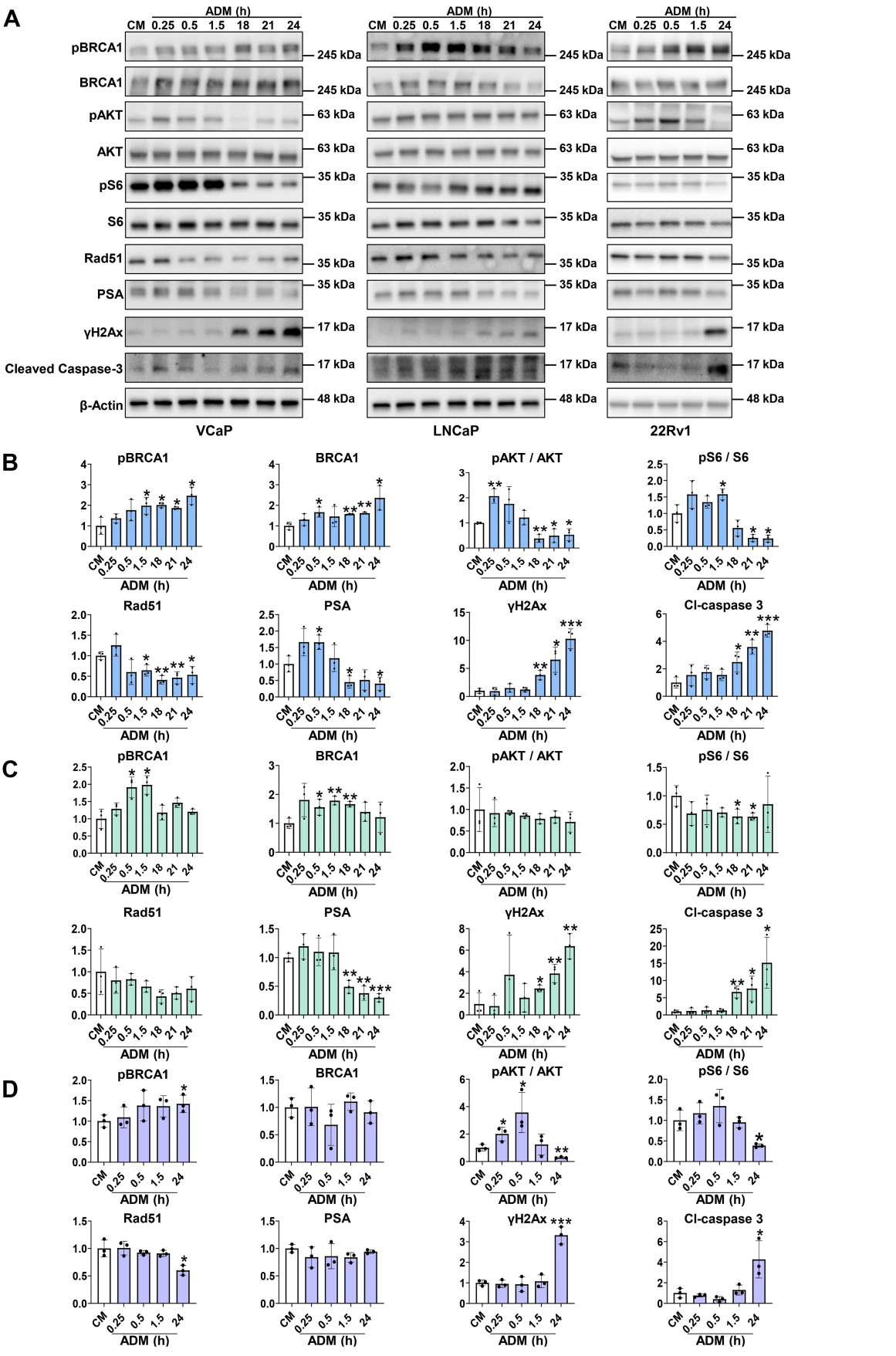

Figure 2 Legend on next page.

primarily by DNA-damaging processes, independent of AR.

ADT induces DNA damage and BRCA1 phosphorylation in murine VCaP xenografts

To assess the reproducibility of our findings *in vivo*, we used a murine VCaP xenograft model of ADT (Figure 3A). Tumor volume and PSA were measured weekly, and after sacrifice, tumor weight as well as tumor tissue section area were measured. As expected, trends suggesting tumor regression and concurrent PSA decline were observed in response to ADT (supplementary material, Figure S3A,B), suggesting that reduced AR may lead to cell death in xenograft tumors (supplementary material, Figure S3C,D).

Next, we performed IHC on xenograft tumors using γH2Ax, pBRCA1, Rad51, and pS6 antibodies and measured relative areas of strong positive staining (Figure 3B). We observed induced γH2Ax, increased pBRCA1, decreased Rad51, and decreased pS6 based on the staining of the VCaP xenografts from day 2, matching our earlier VCaP cell results (Figure 2A,B), indicating that these proteins were indeed regulated *in vivo* (Figure 3C,D; supplementary material, Figures S3E and S4A). Samples from day 5 showed similar trends, albeit with greater variability, which may have resulted from the most severely affected cells perishing by this later timepoint. A massive sudden DNA damage event, if inadequately resolved, would likely have resulted in cell death. Consequently, the surviving cells at later timepoints may have become enriched for unaffected cells, potentially contributing to the observed variability. Importantly, pBRCA1 staining negatively correlated with PSA, further evidencing that AR activity is inversely associated with BRCA1 (Figure 3E). Interestingly, the correlation was also evident when analyzing the intact group separately, suggesting that BRCA1 regulation by AR activity was significant already without intervention (supplementary material, Figure S4B). Taken together, these data supported our finding that AD induced DNA damage and increased BRCA1 activation.

ADT induces expression and phosphorylation of BRCA1 and increases DNA damage in clinical PCa specimens

We further investigated whether the protein expression of BRCA1, pBRCA1, and γH2Ax is altered in clinical PCa tumors upon ADT, similar to our *in vitro* and *in vivo* models. Paired samples from 11 PCa patients before (all primary tumors) and after ADT (64% from metastases, 64% CRPC, Table 1) were analyzed by IHC using the antibodies against BRCA1, pBRCA1, and γH2Ax (Figure 3F; supplementary material, Figure S5). Based on scoring of IHC staining, BRCA1, pBRCA1, and γH2Ax were upregulated post-ADT in all cases except one, suggesting that DNA damage and active phospho-BRCA1 became enriched post-ADT and may have contributed to the development of resistance to ADT.

AD induces BRCA1 together with the antioxidant transcription factor NRF2

We investigated previously published transcriptomic data from *BRCA1*-silenced PCa cells [22]. To assess which processes were potentially lost during BRCA1 repression and promoted during BRCA1 activation, we focused on genes downregulated in *BRCA1*-silenced cells (Figure 4A–C). We observed that the differentially expressed genes showed the highest association with gene sets relating to biological processes and hallmarks that already had an established association with *BRCA1*. Notably, the number one oncogenic gene set associated with changes seen in this PCa cell line was a set of NRF2-regulated genes [29,30] (Figure 4C). AD has been suggested to increase the expression of antioxidant markers and ROS in PCa cells, which is linked to castration resistance [31,32]. We hypothesized that ROS could, in part, be linked to the observed BRCA1 phosphorylation as a universal response to AD because the BRCA1 phosphorylation site activator ATM is also directly activated by ROS [33]. NRF2 is a well-attributed master transcription factor for antioxidant synthesis [5,34]. BRCA1 was previously reported to regulate NRF2-dependent antioxidant signaling by physically interacting with NRF2 and promoting its stability and activation [3–5]. Here, we observed that 5 days of ADM upregulated both BRCA1 and NRF2 expression (Figure 4D). Furthermore, ADM-induced BRCA1 expression was blocked upon *NFE2L2* (NRF2) knockdown (Figure 4E). These data suggested that NRF2 was indeed involved in BRCA1 regulation in response to AD.

The BRCA1-NRF2 regulatory axis regulates PCa cell spheroidal growth

Next, we examined the effects of modified *BRCA1* expression in PCa cells. We chose to use siRNA for gene silencing, given its ability to partially retain protein expression, thereby protecting cell viability from the complete loss of essential functions of BRCA1. After silencing *BRCA1*, no difference was observed in the viability of LNCaP cells in 2D culture (Figure 5A); however, a 54.5% smaller size was observed for LNCaP cell spheroids (Figure 5B–D). In AR-negative

Figure 2. AD induces DNA damage and cell death in PCa. (A) Representative western blotting depicting expression of key HR components, AR targets, and markers of PI3K-Akt/mTOR signaling, DNA damage, and apoptosis with loading control expression in VCaP, LNCaP, and 22Rv1 cells subjected to ADM (0.25–24 h) along with control (normal culture media, CM). (B–D) Bar graphs depicting pooled western blot densitometry results of three biological repeats. The mean and SD from three experiments are represented as a bar graph (*$p < 0.05$, **$p < 0.01$, and ***$p < 0.001$ as determined by Student's *t*-test).

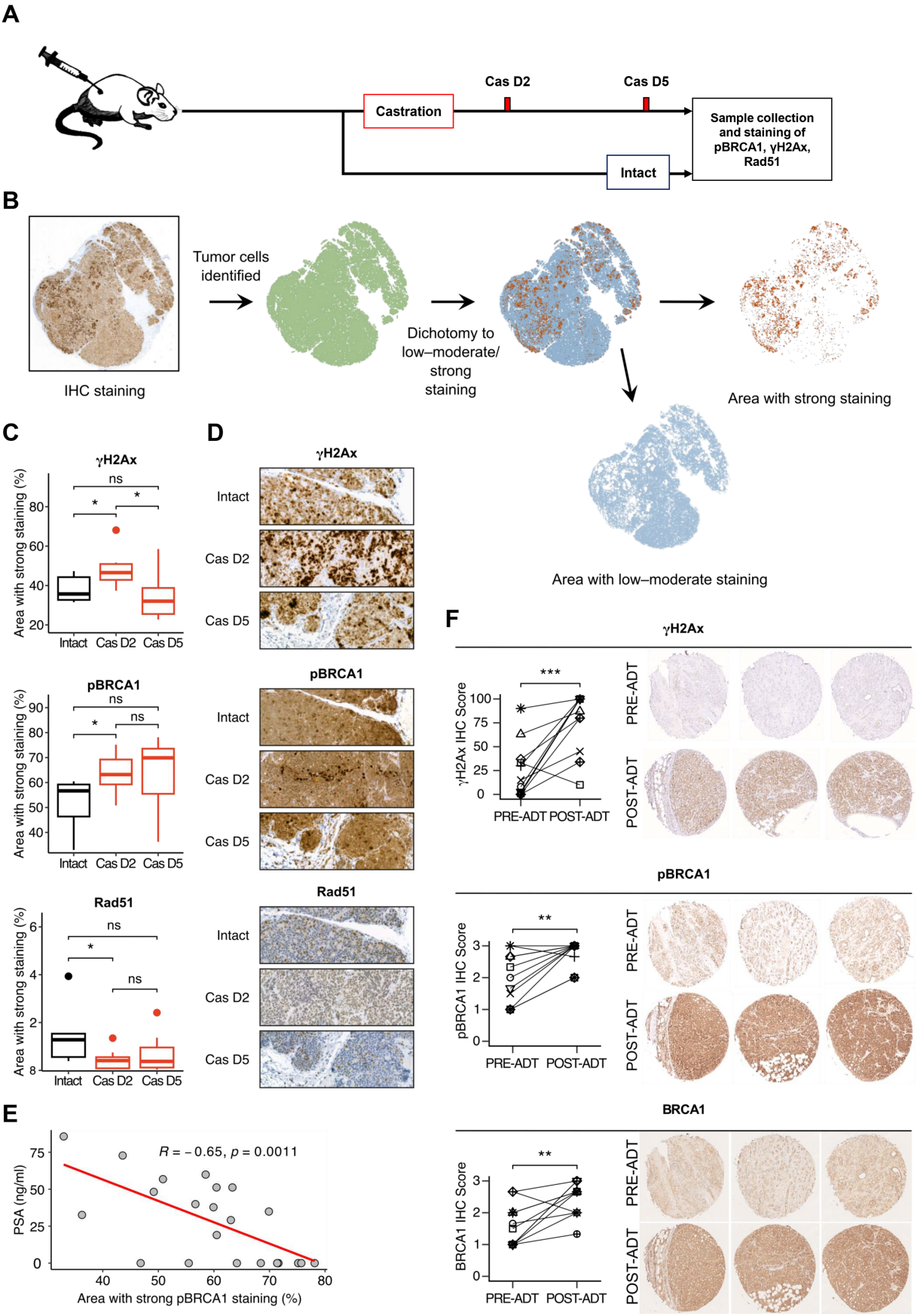

Figure 3 Legend on next page.

Table 1. Baseline characteristics of the patients.

Age (years) at initial diagnosis of prostate cancer	
Median (range)	58 (54–79)
Gleason score at initial diagnosis of prostate cancer (*n*, %)	
7	4 (36)
8	3 (27)
9	4 (36)
PSA (µg/l) level at primary diagnosis	
Median (range)	13 (3.9–57)
Initial treatment (*n*, %)	
ADT + RT	3 (27)
Surgery + ADT	6 (54)
ADT only	2 (18)
Time since start of ADT to post-ADT sample (months)	
Median (range)	66 (18–107)
Other hormonal treatments after ADT (*n*, %)	
AR inhibitors	11 (100)
Abiraterone	1 (9)
Origin of post-ADT sample (*n*, %)	
Prostate (TURP)	4 (36)
Metastasis	7 (64)
Clinical castration resistance at post-ADT sample (*n*, %)	
CRPC	7 (64)
No[a]	4 (36)
Metastases[b] (*n*, %)	
None	1 (9)
Bone only	2 (18)
Lymph node only	1 (9)
Bone + lymph node or visceral only	6 (54)
Visceral	5 (45)

Abbreviation: ADT, androgen deprivation therapy; CRPC, castration-resistant prostate cancer; PSA, prostate-specific antigen; RT, radiotherapy; TURP, transurethral resection of the prostate.
[a]Relapse after ADT but no CRPC at the time of post-ADT sample.
[b]At the time of post-ADT sample.

PC-3 cells, *BRCA1* knockdown had no significant effect on confluence of cells in 2D culture, but the spheroids in 3D were 84.5% smaller (supplementary material, Figure S6A–E), similar to LNCaP cells. Taken together, this suggested that the function of BRCA1 was more important for PCa cells in the 3D culture context, enriched with ROS [35,36].

Interestingly, silencing *NFE2L2* reduced spheroid size in the LNCaP cells, similar to silencing *BRCA1* (Figure 5E). Moreover, silencing of *BRCA1* in LNCaP cells downregulated the protein products of NRF2 target genes, NQO1 and FTH1, in 3D culture (Figure 5F). In PC-3 cells, silencing of *BRCA1* equally led to downregulation of NRF2 targets, as well as NRF2 itself (supplementary material, Figure S6F). These results suggested a bidirectional regulatory axis for BRCA1 and NRF2 in PCa cells.

Whereas *BRCA1* is well known to be mutated in PCa and is among the PCa predisposing DDR genes, we found that amplified *BRCA1* was also observed at similar rates compared to mutations across published cohorts [6,7,9,11,37,38] (Figure 5G). Furthermore, we found that neuroendocrine PCa (NEPC) features were more common in patients with high *BRCA1* expression levels in metastatic CRPC [6] (Figure 5H). This and the fact that BRCA1 was expressed in all widely used PCa cell lines suggested that BRCA1 expression is still prevalent in non-BRCA1 mutated PCa.

We examined *BRCA1* expression in public patient datasets and found that high *BRCA1* expression was correlated with shorter progression- and disease-free survival in TCGA and MSK cohorts, respectively, whereas the effect on overall survival was not significant in TCGA [18] (Figure 5I,J). Furthermore, we found that high expression of *BRCA1* and several known NRF2-regulated genes are associated with worse overall survival in metastatic CRPC patients in the SU2C dataset [6] (Figure 5K; supplementary material, Table S5) [6]. Taken together, these data suggest that high *BRCA1* expression is prevalent in progressing PCa. The frequencies of *BRCA1* mutations were low in the analyzed cohorts, and consequently, the low *BRCA1* groups do not represent the aggressive phenotype of genomic *BRCA1* loss. Therefore, it is plausible that the observed survival correlations were a consequence of AR activation-mediated modulation of the BRCA1-NRF2 regulatory axis. Thus, we conclude that the tumor suppressor gene *BRCA1* is expressed and activated by ADT for its antioxidant properties and repressed during hyperactive AR signaling, putatively exacerbating progression via the loss of its tumor suppressive function (Figure 6).

Discussion

Preclinical studies in PCa have suggested that AR signaling regulates DDR [12–16]. However, findings from these studies are in part contradictory, and the regulation of *BRCA1* by natural ligands of AR or ADT has not been reported [12–16]. Moreover, the low frequency of *BRCA1* mutations observed in PCa compared to the high frequency observed in other HR-prone cancers, such as breast and ovarian cancer, remains unexplained [10]. Therefore, we sought to systematically characterize the regulation of

Figure 3. BRCA1 expression is retained and phosphorylated in response to ADT. (A) A schematic figure representing the sample generation process of Intact, Cas D2, and Cas D5 VCaP mice xenograft tumors. (B) A schematic figure representing the analysis pipeline in QuPath for scoring the IHC staining. (C) Boxplots depicting the percentages of strong IHC staining of pBRCA1, Rad51, and γH2Ax in VCaP xenograft tumors (ns = not significant and $*p < 0.05$ as determined by Mann–Whitney *U*-test). (D) Representative images of IHC staining in VCaP xenograft tumor. High-resolution versions of the images shown are provided in the supplementary material, Figure S4A. (E) Scatterplots depicting Pearson correlation between PSA concentration (ng/ml) and the percentage of strong IHC staining of BRCA1 in VCaP xenograft tumors. (F) Representative IHC staining and scoring of γH2Ax, pBRCA1, and BRCA1 from PCa samples obtained from the same patients before and after starting ADT (representative images shown, total $n = 11$ patients, $*p < 0.05$ and $**p < 0.01$ as determined by Student's *t*-test). High-resolution versions of the images shown are provided in the supplementary material, Figure S5.

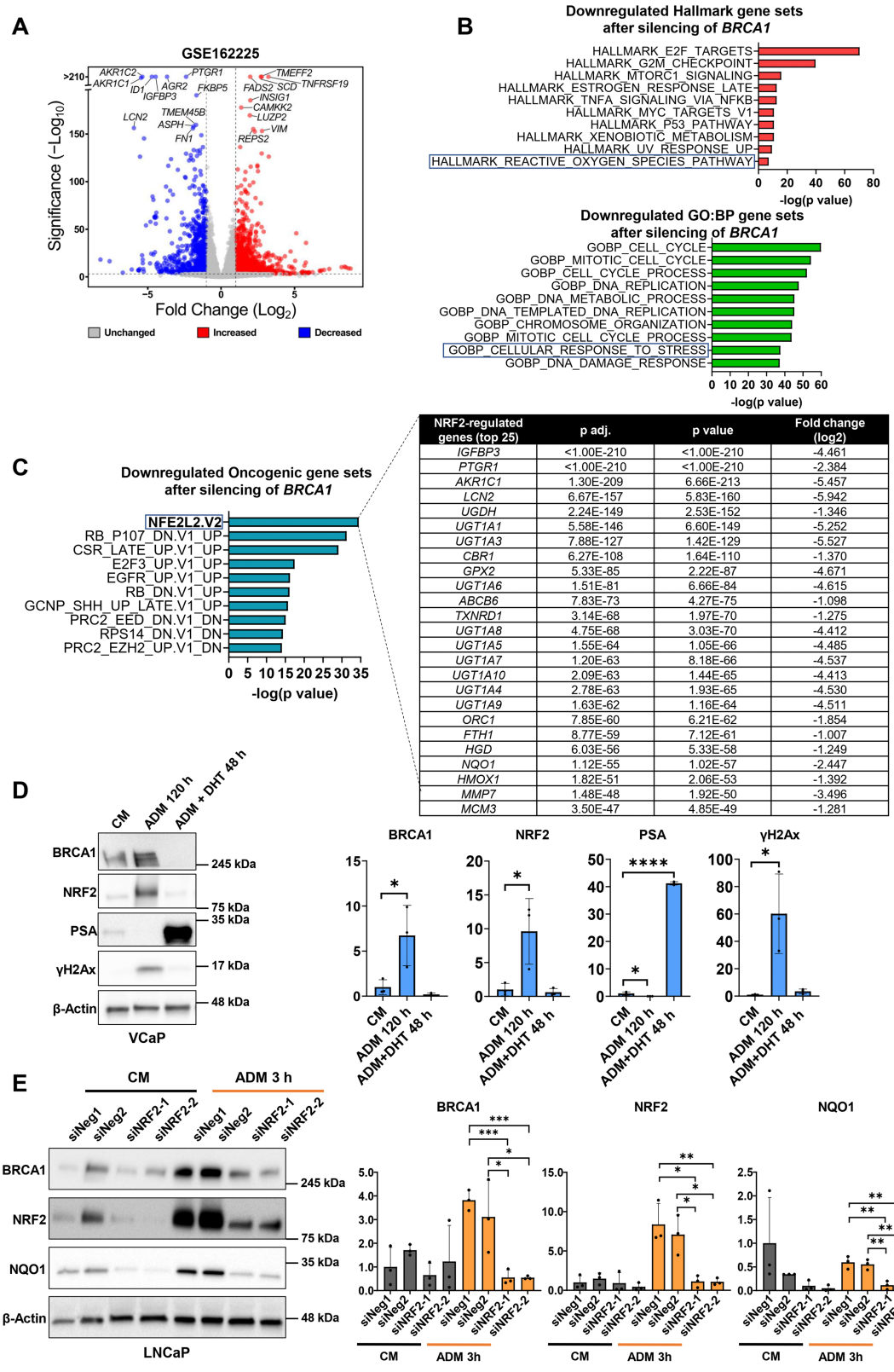

NRF2-regulated genes (top 25)	p adj.	p value	Fold change (log2)
IGFBP3	<1.00E-210	<1.00E-210	-4.461
PTGR1	<1.00E-210	<1.00E-210	-2.384
AKR1C1	1.30E-209	6.66E-213	-5.457
LCN2	6.67E-157	5.83E-160	-5.942
UGDH	2.24E-149	2.53E-152	-1.346
UGT1A1	5.58E-146	6.60E-149	-5.252
UGT1A3	7.88E-127	1.42E-129	-5.527
CBR1	6.27E-108	1.64E-110	-1.370
GPX2	5.33E-85	2.22E-87	-4.671
UGT1A6	1.51E-81	6.66E-84	-4.615
ABCB6	7.83E-73	4.27E-75	-1.098
TXNRD1	3.14E-68	1.97E-70	-1.275
UGT1A8	4.75E-68	3.03E-70	-4.412
UGT1A5	1.55E-64	1.05E-66	-4.485
UGT1A7	1.20E-63	8.18E-66	-4.537
UGT1A10	2.09E-63	1.44E-65	-4.413
UGT1A4	2.78E-63	1.93E-65	-4.530
UGT1A9	1.63E-62	1.16E-64	-4.511
ORC1	7.85E-60	6.21E-62	-1.854
FTH1	8.77E-59	7.12E-61	-1.007
HGD	6.03E-56	5.33E-58	-1.249
NQO1	1.12E-55	1.02E-57	-2.447
HMOX1	1.82E-51	2.06E-53	-1.392
MMP7	1.48E-48	1.92E-50	-3.496
MCM3	3.50E-47	4.85E-49	-1.281

Figure 4. BRCA1 associates with NRF2-mediated antioxidant signaling during AD-induced oxidative stress in PCa. (A) Volcano plot depicting differentially regulated genes in LNCaP cells after silencing *BRCA1*. (B) Plots of significantly downregulated Hallmark gene sets and GO:BP gene sets from MSigDB after silencing *BRCA1* in LNCaP cells (C) Significantly downregulated Oncogenic gene sets from MSigDB after silencing *BRCA1* in LNCaP cells. The Table highlights the top 25 downregulated genes after silencing *BRCA1*, in the gene set NFE2L2.V2, based on genes downregulated after silencing *NFE2L2*. (D) Western blotting and bar graphs of pooled western blotting densitometry depicting BRCA1, NRF2, PSA, γH2Ax, and loading control expression in VCaP cells subjected to vehicle (methanol), 5 days of ADM, and 48 h of DHT (10 nM) after 3 days of ADM treatment. (E) Western blotting and bar graphs of pooled western blotting densitometry depicting BRCA1, NRF2, NQO1, and loading control expression after transfection with siNeg1, siNeg2, siNRF2-1, and siNRF2-2 with or without ADM (3 h) in LNCaP cells. The mean and SD from three experiments are represented as bar graph, unless otherwise indicated (ns = not significant, *$p < 0.05$, and **$p < 0.01$ as determined by Student's *t*-test).

BRCA1 by AR and explore the functions of BRCA1 in PCa.

Our results demonstrate that AR activation by ligand mediates the repression of *BRCA1* transcription. The inverse correlation between AR activation and BRCA1 expression was further reinforced by our mouse xenograft data and *in silico* analyses. *BRCA1* has been suggested to be repressed by Id4, the E2F family of

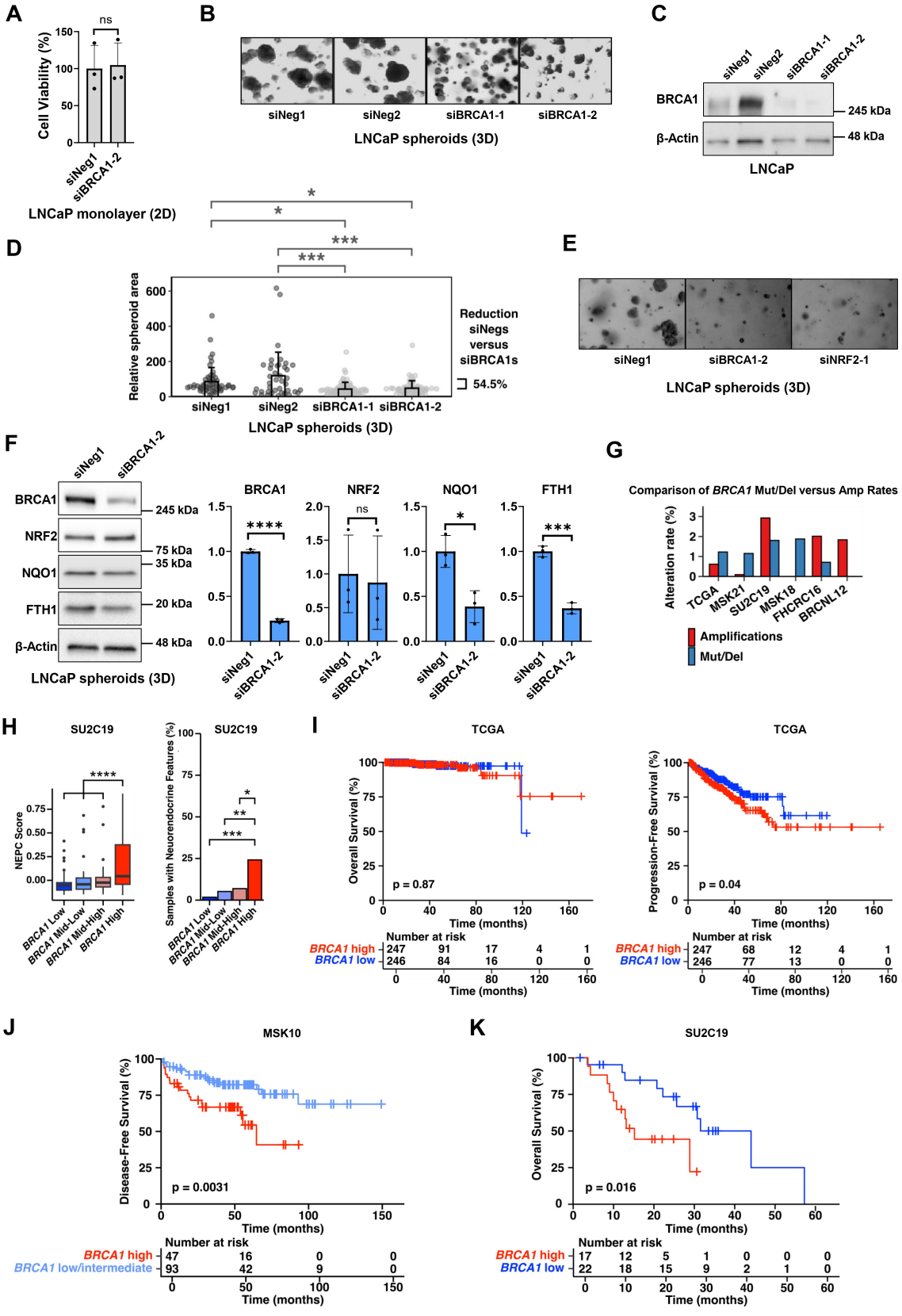

Figure 5 Legend on next page.

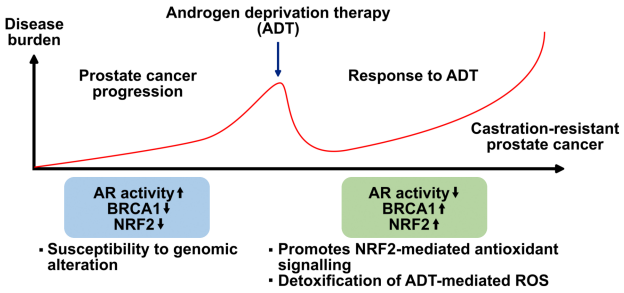

Figure 6. PCa uses AR to repress the BRCA1 tumor suppressor function and to hijack the BRCA1-NRF2 regulatory axis in ROS defense. A schematic diagram depicting how the alternating states of AR activation, dynamically regulated by PCa progression and response to ADT, result in reduced caretaker activity of BRCA1 or improved ROS defense via the modulation of BRCA1-NRF2 regulatory axis in PCa.

transcription factors, Slug, and microRNAs [39–42]. This suggests that the AR may regulate or interact with these or other yet-unidentified repressors or that it directly represses *BRCA1*. The frequency of *BRCA1* mutations found in breast and ovarian cancer is high compared to other cancer types. This has been hypothesized to result from other tissues not surviving without BRCA1 expression [43]. Our finding demonstrating that *BRCA1* is repressed under AR activation provides a rationale for the hypothesis that the AR-driven PCa repression may transiently impair the tumor suppressor function of BRCA1, thus supporting the accumulation of oncogenic alterations. Therefore, the already impaired tumor suppressor gene function would provide no selective pressure toward somatic *BRCA1* mutations. On the other hand, we found that ADT activates *BRCA1* to defend against ROS, which may, in turn, select against somatic *BRCA1* mutations.

Interestingly, ADM induced DNA damage and apoptosis, while simultaneously increasing BRCA1 expression or phosphorylation independently of AR activation. This suggested that BRCA1 phosphorylation might be more sensitive towards other AD-induced processes, such as ROS. Alternatively, the putative dephosphorylation or inhibition of BRCA1 phosphorylation may require the nuclear localization of domains that are absent in non-full-length AR-V7 present in 22Rv1, as full-length AR remains cytoplasmic during AD. Furthermore, we demonstrated that AD similarly induced both BRCA1 and NRF2, and silencing *BRCA1* or *NFE2L2* resulted in a reciprocal downregulation in specific conditions such as AD, organoid culture, or AR-negative cells, which suggests the involvement of ROS. AD induces ROS-mediated oxidative stress, and BRCA1 regulates and interacts with NRF2 [3–5,33,34]. Our data revealed that the BRCA1-NRF2 regulatory axis is active in PCa and potentially hijacked by CRPC to defend against toxic ROS.

Patient data suggested that high *BRCA1* expression was linked to a poor prognosis of PCa patients. High *BRCA1* levels were also found to be associated with neuroendocrine PCa features. Interestingly, a recent patient-derived organoid study showed increased DDR gene expression in neuroendocrine PCa samples, which suggests that AR independence is linked to the increased function of some DDR genes [26]. This complements our finding that, while *BRCA1* appears to be suppressed in association with AR activation in AR-driven PCa, its expression remains unaffected in less AR-dependent PCa.

In conclusion, our study sheds light on the role of the tumor suppressor BRCA1 in PCa. Inherited *BRCA1* mutations are associated with a predisposition for aggressive PCa, but most PCa patients still carry intact *BRCA1*. We demonstrate that AR mediates *BRCA1* repression and that ADT activates, rather than suppresses, BRCA1 expression in PCa. Thus, we propose that BRCA1 plays two distinct roles in PCa when not mutated: first, as a repressed tumor suppressor, thus putatively promoting tumorigenesis and progression and, in the later stage, through ADT-mediated activation, to protect tumor cells against ROS by inducing NRF2 and its targets.

Acknowledgments

We thank Sinikka Collanus and the Histology core facility of the Institute of Biomedicine, University of Turku, for their assistance with IHC. We thank Minna Santanen, Jukka Karhu, and Barbara Ramos Artigot for their

Figure 5. BRCA1 supports organotypic 3D spheroid growth of PCa cells. (A) Plots representing cell viability (%) of LNCaP cells with or without *BRCA1* knockdown. (B) Representative brightfield images from day 7 in 3D culture of LNCaP cells treated with siNeg1, siNeg2, siBRCA1-1, or siBRCA1-2. (C) Western blotting depicting BRCA1 and loading control expression 48 h after transfection for 3D culture in LNCaP cells. (D) Plots depicting relative 3D spheroid area in brightfield images for LNCaP cells on day 7 of 3D culture. (E) Representative brightfield images from day 5 in a 3D culture of LNCaP cells treated with siNeg1, siBRCA1-2, or siNRF2-1. (F) Western blotting and bar graphs depicting the expression of NRF2 and its targets NQO1 and FTH1 along with BRCA1 and loading control expression after 5 days of 3D culture in LNCaP cells with or without *BRCA1* knockdown. (G) Plots representing *BRCA1* alterations in PCa patient datasets TCGA [37], MSK21 [38], SUC19 [6], MSK18 [7], FHCRC16 [9], and BRCNL12 [11]. (H) Plots representing the presence of histological NEPC features and transcript-based NEPC score in PCa patients stratified by *BRCA1* mRNA expression quartiles analyzed from the SU2C cohort. (I) Kaplan–Meier plot depicting overall survival and progression-free survival of PCa patients stratified by *BRCA1* mRNA medians analyzed from the TCGA PanCancer Atlas cohort. (J) Kaplan–Meier plot depicting disease-free survival of PCa patients stratified by *BRCA1* mRNA expression tertiles, comparing the highest tertile to the combined lower tertiles analyzed from the MSK Cancer Cell 2010 cohort. (K) Kaplan–Meier plot depicting overall survival of PCa patients stratified by *BRCA1* mRNA quartiles, comparing the highest quartile to the lowest quartile analyzed from the SU2C cohort. Statistical significance of the Kaplan–Meier survival curves was determined using the log-rank test. The mean and SD from three experiments are represented as bar graphs (*$p < 0.05$, **$p < 0.01$, and ***$p < 0.001$ as determined by Student's *t*-test).

excellent technical assistance. We also thank the Turku Center for Disease Modeling (TCDM), Guillermo Martinez Nieto, and Petra Sipilä for providing their expertise in generating mouse xenograft models. We thank Syeda Afshan for providing us with synthetic androgen R1881 for the studies. The results here are partly based upon data generated by the TCGA Research Network: https://www.cancer.gov/tcga. This study was supported by grants from the Academy of Finland, Finnish Medical Foundation, Cancer Foundation Finland, Cancer Society of Southwest Finland, Turku University Foundation, Hospital District of Southwest Finland, Sigrid Jusélius Foundation, Paulo Foundation, Instrumentarium Foundation, Finnish National Agency for Education (EDUFI) and Turku Doctoral Programme of Molecular Medicine. Open access publishing facilitated by Turun yliopisto, as part of the Wiley - FinELib agreement.

Author contributions statement

SS, VV, AK and MS designed the study, conceived the experiments, and analyzed the data. SS, VV and AK prepared the figures. SS, VV, AK, AL and MT carried out experiments. SS, VV, AK and MS designed the *in silico* analyses. MP designed the xenograft experiment. PT designed the human IHC analyses and provided the samples. GW analyzed the human IHC samples. SS, VV and MS wrote the article and all authors commented on and approved the final version. MS acquired the funding and supervised the study.

Data availability statement

Raw data generated in this study are available upon reasonable request to the corresponding author.

References

1. Venkitaraman AR. Cancer susceptibility and the functions of BRCA1 and BRCA2. *Cell* 2002; **108**: 171–182.
2. van Vugt MA, Parkes EE. When breaks get hot: inflammatory signaling in BRCA1/2-mutant cancers. *Trends Cancer* 2022; **8**: 174–189.
3. Bae I, Fan S, Meng Q, *et al*. BRCA1 induces antioxidant gene expression and resistance to oxidative stress. *Cancer Res* 2004; **64**: 7893–7909.
4. Gorrini C, Baniasadi PS, Harris IS, *et al*. BRCA1 interacts with Nrf2 to regulate antioxidant signaling and cell survival. *J Exp Med* 2013; **210**: 1529–1544.
5. de la Vega MR, Chapman E, Zhang DD. NRF2 and the hallmarks of cancer. *Cancer Cell* 2018; **34**: 21–43.
6. Abida W, Cyrta J, Heller G, *et al*. Genomic correlates of clinical outcome in advanced prostate cancer. *Proc Natl Acad Sci U S A* 2019; **116**: 11428–11436.
7. Armenia J, Wankowicz SA, Liu D, *et al*. The long tail of oncogenic drivers in prostate cancer. *Nat Genet* 2018; **50**: 645–651.
8. Robinson D, Van Allen EM, Wu Y-M, *et al*. Integrative clinical genomics of advanced prostate cancer. *Cell* 2015; **161**: 1215–1228.
9. Kumar A, Coleman I, Morrissey C, *et al*. Substantial interindividual and limited intraindividual genomic diversity among tumors from men with metastatic prostate cancer. *Nat Med* 2016; **22**: 369–378.
10. Nguyen L, Martens WM, Van Hoeck A, *et al*. Pan-cancer landscape of homologous recombination deficiency. *Nat Commun* 2020; **11**: 5584.
11. Barbieri CE, Baca SC, Lawrence MS, *et al*. Exome sequencing identifies recurrent SPOP, FOXA1 and MED12 mutations in prostate cancer. *Nat Genet* 2012; **44**: 685–689.
12. Goodwin JF, Schiewer MJ, Dean JL, *et al*. A hormone–DNA repair circuit governs the response to genotoxic insult. *Cancer Discov* 2013; **3**: 1254–1271.
13. Li L, Karanika S, Yang G, *et al*. Androgen receptor inhibitor–induced "BRCAness" and PARP inhibition are synthetically lethal for castration-resistant prostate cancer. *Sci Signal* 2017; **10**: eaam7479.
14. Asim M, Tarish F, Zecchini HI, *et al*. Synthetic lethality between androgen receptor signalling and the PARP pathway in prostate cancer. *Nat Commun* 2017; **8**: 374.
15. Polkinghorn WR, Parker JS, Lee MX, *et al*. Androgen receptor signaling regulates DNA repair in prostate cancers. *Cancer Discov* 2013; **3**: 1245–1253.
16. Hasterok S, Scott TG, Roller DG, *et al*. The androgen receptor does not directly regulate the transcription of DNA damage response genes. *Mol Cancer Res* 2023; **21**: 1329–1341.
17. Grasso CS, Wu Y-M, Robinson DR, *et al*. The mutational landscape of lethal castration-resistant prostate cancer. *Nature* 2012; **487**: 239–243.
18. Taylor BS, Schultz N, Hieronymus H, *et al*. Integrative genomic profiling of human prostate cancer. *Cancer Cell* 2010; **18**: 11–22.
19. Virtanen V, Paunu K, Kukkula A, *et al*. Glucocorticoid receptor-induced non-muscle caldesmon regulates metastasis in castration-resistant prostate cancer. *Oncogene* 2023; **12**: 42.
20. Huhtaniemi R, Oksala R, Knuuttila M, *et al*. Adrenals contribute to growth of castration-resistant VCaP prostate cancer xenografts. *Am J Pathol* 2018; **188**: 2890–2901.
21. Hoefer J, Kern J, Ofer P, *et al*. SOCS2 correlates with malignancy and exerts growth-promoting effects in prostate cancer. *Endocr Relat Cancer* 2013; **21**: 175.
22. Han H, Wang Y, Curto J, *et al*. Mesenchymal and stem-like prostate cancer linked to therapy-induced lineage plasticity and metastasis. *Cell Rep* 2022; **39**: 110595.
23. Goedhart J, Luijsterburg MS. VolcaNoseR is a web app for creating, exploring, labeling and sharing volcano plots. *Sci Rep* 2020; **10**: 20560.
24. Tsherniak A, Vazquez F, Montgomery PG, *et al*. Defining a cancer dependency map. *Cell* 2017; **170**: e516.
25. Gao D, Vela I, Sboner A, *et al*. Organoid cultures derived from patients with advanced prostate cancer. *Cell* 2014; **159**: 176–187.
26. Anselmino N, Labanca E, Shepherd PD, *et al*. Integrative molecular analyses of the MD Anderson prostate cancer patient-derived xenograft (MDA PCa PDX) series. *Clin Cancer Res* 2024; **30**: 2272–2285.
27. Gerhauser C, Favero F, Risch T, *et al*. Molecular evolution of early-onset prostate cancer identifies molecular risk markers and clinical trajectories. *Cancer Cell* 2018; **34**: 996–1011.e8.
28. Cortez D, Wang Y, Qin J, *et al*. Requirement of ATM-dependent phosphorylation of brca1 in the DNA damage response to double-strand breaks. *Science* 1999; **286**: 1162–1166.
29. Malhotra D, Portales-Casamar E, Singh A, *et al*. Global mapping of binding sites for Nrf2 identifies novel targets in cell survival response through ChIP-seq profiling and network analysis. *Nucleic Acids Res* 2010; **38**: 5718–5734.
30. Kim JW, Botvinnik OB, Abudayyeh O, *et al*. Characterizing genomic alterations in cancer by complementary functional associations. *Nat Biotechnol* 2016; **34**: 539–546.
31. Shiota M, Song Y, Takeuchi A, *et al*. Antioxidant therapy alleviates oxidative stress by androgen deprivation and prevents conversion

from androgen dependent to castration resistant prostate cancer. *J Urol* 2012; **187**: 707–714.
32. Ferrari N, Granata I, Capaia M, *et al*. Adaptive phenotype drives resistance to androgen deprivation therapy in prostate cancer. *Cell Commun Signal* 2017; **15**: 1–14.
33. Guo Z, Kozlov S, Lavin MF, *et al*. ATM activation by oxidative stress. *Science* 2010; **330**: 517–521.
34. Sies H, Jones DP. Reactive oxygen species (ROS) as pleiotropic physiological signalling agents. *Nat Rev Mol Cell Biol* 2020; **21**: 363–383.
35. Rybkowska P, Radoszkiewicz K, Kawalec M, *et al*. The metabolic changes between monolayer (2D) and three-dimensional (3D) culture conditions in human mesenchymal stem/stromal cells derived from adipose tissue. *Cells* 2023; **12**: 178.
36. Liu Q, Zhang Z, Liu Y, *et al*. Cancer cells growing on perfused 3D collagen model produced higher reactive oxygen species level and were more resistant to cisplatin compared to the 2D model. *J Appl Biomater Funct Mater* 2018; **16**: 144–150.
37. ICGC/TCGA Pan-Cancer Analysis of Whole Genomes Consortium. Pan-cancer analysis of whole genomes. *Nature* 2020; **578**: 82–93.
38. Nguyen B, Fong C, Luthra A, *et al*. Genomic characterization of metastatic patterns from prospective clinical sequencing of 25,000 patients. *Cell* 2022; **185**: 563–575.e11.
39. Beger C, Pierce LN, Krüger M, *et al*. Identification of Id4 as a regulator of BRCA1 expression by using a ribozyme-library-based inverse genomics approach. *Proc Natl Acad Sci U S A* 2001; **98**: 130–135.
40. Bindra RS, Gibson SL, Meng A, *et al*. Hypoxia-induced down-regulation of BRCA1 expression by E2Fs. *Cancer Res* 2005; **65**: 11597–11604.
41. Wu Z-Q, Li X-Y, Hu CY, *et al*. Canonical Wnt signaling regulates slug activity and links epithelial–mesenchymal transition with epigenetic breast cancer 1, early onset (BRCA1) repression. *Proc Natl Acad Sci U S A* 2012; **109**: 16654–16659.
42. Chang S, Sharan SK. BRCA1 and microRNAs: emerging networks and potential therapeutic targets. *Mol Cells* 2012; **34**: 425–432.
43. Elledge SJ, Amon A. The BRCA1 suppressor hypothesis: an explanation for the tissue-specific tumor development in BRCA1 patients. *Cancer Cell* 2002; **1**: 129–132.

SUPPLEMENTARY MATERIAL ONLINE

Supplementary materials and methods

Figure S1. Association between AR and BRCA1 in androgen-dependent PCa

Figure S2. Analysis of additional DDR markers in AD conditions and influence of mTOR signaling pathway in HR repair pathway in PCa

Figure S3. Representation of key attributes of Intact, Cas D2, and Cas D5 tumors obtained from VCaP mice xenografts

Figure S4. VCaP xenograft high-resolution IHC images and correlation between PSA levels and BRCA1 staining intensity

Figure S5. PCa patient sample high-resolution IHC images

Figure S6. Association of BRCA1 with organotypic growth and antioxidant signaling pathway in PCa

Table S1. List of siRNAs used in this study

Table S2. List of antibodies used in this study

Table S3. List of TaqMan probes used in this study

Table S4. List of the top 500 downregulated genes in *BRCA1*-silenced LNCaP cells

Table S5. Association of BRCA1 and NRF2 signaling pathway in PCa